

MODEL BASED PREDICTIVE CONTROL OF UNDERACTUATED NONLINEAR MECHATRONICAL SYSTEMS

Ádám VARGA and Béla LANTOS

Department of Control Engineering and Information Technology
Budapest University of Technology and Economics
H-1117 Budapest, Magyar Tudósok krt. 2, Hungary
e-mail: avarga@seeger.iit.bme.hu, lantos@iit.bme.hu

Received: April 15, 2005

Abstract

The paper deals with model predictive control of underactuated nonlinear mechatronical systems along known reference path. It generalizes the state space predictive control algorithm of linear time invariant (LTI) systems to linearized time variant (LTV) systems. An algorithm is presented, which calculates the LTV model online from the nonlinear model along the reference trajectory. The LTV is then used in the framework of the predictive control to find the optimal control in closed analytical form without using online optimum search in the moving horizon. After MATLAB-based simulation results of the algorithm, successful test experiments were performed for the predictive control of a real inverted pendulum system, both in the swinging up and upper stabilization phases.

Keywords: model predictive control, linearized time variant systems, inverted pendulum.

1. Introduction

Model based predictive control is a popular method especially in the process industry where relatively slow process models allow online optimization. Linear predictive control is well elaborated both in frequency (operator) domain [1, 3] and state space [2, 3]. Depending on the type of constraints optimal prediction systems lead to Quadratic Programming (QP) or Nonlinear Programming (NP) based on Sequential Optimization which are well supported by existing softwares (e.g. Optimization Toolbox in MATLAB).

For nonlinear systems recent methods are usually based on new optimum seeking methods suited for the predictive control problem or traditional analytical optimum conditions and gradient based optimization techniques [4, 5]. Basis for the later ones is a general form of the Lagrange multiplicator rule which is also valid in Banach spaces [3].

Typical finite horizon nonlinear predictive control problems in discrete time lead to optimization in finite dimensional space where the variables are

$x = \{x_i\}_{i=0}^N$ and $u = \{u_i\}_{i=0}^{N-1}$, the optimality criterion is

$$\begin{aligned} F_0(x, u) &= \frac{1}{2} \sum_{i=0}^{N-1} [\langle Q_i x_i, x_i \rangle + \langle R_i u_i, u_i \rangle] + \frac{1}{2} \langle Q_N x_N, x_N \rangle \\ &=: \sum_{i=0}^{N-1} L_i(x_i, u_i) + \Phi(x_N), \end{aligned} \quad (1)$$

the constraints are the state equation

$$\varphi(x_i, u_i) - x_{i+1} = 0, \quad (2)$$

control set $u_i \in M$ and initial condition $a - x_0 = 0$.

If (x^*, u^*) is the optimal solution then

$$f(x, u) = J'_x(x^*, u^*)x + J'_u(x^*, u^*)u$$

is the derivative of

$$\begin{aligned} J(x, u) &= F_0(x, u) + \langle \lambda_0, a - x_0 \rangle + \langle \lambda_1, \varphi(x_0, u_0) - x_1 \rangle + \cdots + \\ &\quad \langle \lambda_N, \varphi(x_{N-1}, u_{N-1}) - x_N \rangle. \end{aligned}$$

By introducing the Hamiltonian functions as

$$H_i = \langle \lambda_{i+1}, \varphi(x_i, u_i) \rangle + L_i(x_i, u_i),$$

the necessary condition of the optimality results in

$$\begin{aligned} \lambda_N &= Q_N x_N, \\ \lambda_i &= \partial H_i / \partial x_i = Q_i x_i + (\partial \varphi / \partial x_i)^T \lambda_{i+1}, \\ \partial H_i / \partial u_i &= R_i u_i + (\partial \varphi / \partial u_i)^T \lambda_{i+1}, \\ dJ &= \sum_{i=0}^{N-1} \langle \partial H_i / \partial u_i, u_i^* - u_i \rangle \leq 0. \end{aligned} \quad (3)$$

For the control design within the actual horizon first the initial condition x_0 and the approximation of u are needed (the latter may be the solution in the previous horizon shifted to the left).

The optimization repeats the following steps:

1. Solution of the state equations in $x = \{x_i\}_{i=0}^N$.
2. Computation of the Lagrange multipliers λ_i .
3. Computation of the derivatives $\partial H_i / \partial u_i$.
4. Numerical optimization based on gradient type methods (gradient, conjugate gradient, Davidon-Fletcher-Powell etc.) to find $u^* = \{u_i^*\}_{i=0}^{N-1}$.

As it can be seen the nonlinear predictive control is a numerically hard problem whose real time realization is limited on the complexity of the nonlinear system model and the computation speed of the hardware and software architecture. Hence important are methods which can give a pseudo-optimal solution without online optimum search.

Especially important are problems controlling underactuated systems (systems having smaller number of control inputs than the freedom of the system). Typical examples of underactuated mechatronics systems are mobile robots, cranes and the inverted pendulum. For such systems not all pathes are realizable hence reference path design is an important subproblem.

In this context in some sense simpler class is the one of flat systems for which the reference path design can be performed by using the flat outputs of the system. In simplified formulation it means that if $\dot{x} = f(x, u)$ is the dynamic model of the system then there exists a new variable y (the flat output) and finite integers q and p such that $x = \phi_1(y, \dot{y}, \ddot{y}, \dots, y^{(q)}), u = \phi_2(y, \dot{y}, \ddot{y}, \dots, y^{(q+1)})$, $y = \psi_1(x, u, \dot{u}, \dots, u^{(p)})$. For example the 2D crane has flat output $y := (x, z)^T$ where x, z are the coordinates of the load in the plane of the crane. For flat systems the reference path can be chosen in polynomial form between initial and final pose satisfying some smoothness conditions. Unfortunately the inverted pendulum is a non-flat system.

In the paper we concentrate on the model based predictive control of underactuated systems however all the results can be applied also for fully actuated systems like robot manipulators etc.

The sections are organized as follows. Section 2 describes the linearization process and it gives the generalization of the state space prediction control algorithm for LTV systems. Section 3 summarizes the model description of the inverted pendulum and the energy based control concept of Åström and Furuta used in the swinging up phase. Section 4 presents the predictive control results of the real inverted pendulum both in the swinging up and upper stabilization phases.

2. Model Predictive Control of Nonlinear Systems along Given Reference Trajectory for Time Varying Small Perturbations

Well elaborated methods in state space are known for model based predictive control of LTI systems which differ in considering the transients after the moving horizon [3]. Popular methods are the ones of MOSCA and ZHANG [7], RAWLINGS and MUSKE [8], and the LQ based method. ROSSITER, KOUVARATAKIS and RICE [2] suggest also extensions to eliminate numerical instability caused by the large number of addition, subtraction and multiplication operations which appear with increasing length of the moving horizon.

Since predictive control uses optimization in open loop within the actual horizon and applies the first term of the optimal control sequence in closed loop hence stability problems can arise. In order to eliminate the stability problem in

the nonlinear case the techniques of Frozen Riccati Equation (FRE) and Control Lyapunov Function (CLF) can be suggested [6]. Unfortunately their real time realization is time consuming.

For LTI systems more effective methods are possible. MOSCA and ZHANG enlarge the length of the horizon by n steps equal to the dimension of the state vector and prescribe as constraints that the n outputs after the horizon should be zero. Since the inputs are zero outside the horizon (assuming that either the plant contains integrator or the integrator of the controller has been moved into the plant for the design phase, but before application it is removed again back into the controller), hence it is enough to assure that all the future outputs are identically zero within the enlarged horizon. Rawlings and Muske separate the eigenstructure of the state space and prescribe that the state belonging to the unstable system part should be zero at the end of the horizon so that its transient is zero after the horizon, furthermore the squares of the outputs after the horizon will be minimized. The third method prescribe that the system should behave after the horizon as an LQ (linear quadratic) optimal system.

These methods exploit the LTI character of the system therefore their generalization for LTV systems is only possible if some simplification assumptions are made, for example that the prolongation of the last system of the horizon within the full LTV model can describe the system behaviour after the horizon. This assumption is similar to FRE assumption for nonlinear systems. Since by experiences FRE is a bad assumption far away from equilibrium hence we have chosen the approach of Mosca and Zhang which is more suitable for the generalization for LTV systems.

2.1. The Original Mosca–Zhang Method for LTI Systems

Let the LTI system be given in the usual form

$$x_{k+1} = Ax_k + Bu_k, \quad y_k = Cx_k, \quad (4)$$

where $x \in R^n$, $u \in R^r$, $y \in R^m$, and assume that the performance criterion in the actual horizon $[0, N]$ is the quadratic function

$$J = \frac{1}{2} \sum_{i=1}^N \{\|y_i\|^2 + \lambda_i \|u_{i-1}\|^2\} \quad (5)$$

The solution of the state equation is

$$\begin{aligned} x_k &= A^k x_0 + \sum_{j=0}^{k-1} A^{k-(j+1)} Bu_j, \\ y_k &= CA^k x_0 + \sum_{j=0}^{k-1} CA^{k-(j+1)} Bu_j, \end{aligned} \quad (6)$$

which can be summarized in the following form:

$$\begin{pmatrix} y_1 \\ y_2 \\ \vdots \\ y_k \end{pmatrix} = \begin{bmatrix} CA \\ CA^2 \\ \vdots \\ CA^k \end{bmatrix} x_0 + \begin{bmatrix} CB & 0 & \cdots & 0 \\ CAB & CB & \cdots & 0 \\ \vdots & \ddots & \ddots & \vdots \\ CA^{k-1}B & \cdots & CAB & CB \end{bmatrix} \begin{bmatrix} u_0 \\ u_1 \\ \vdots \\ u_{k-1} \end{bmatrix} \quad (7)$$

Assuming integrator either in the plant or the controller the stability condition is satisfied if $x_N = 0$ is guaranteed.

It has a similar effect if $y_i = 0$ and $u_i = 0$ for $i \geq N$, or equivalently $y_i = 0$, $i = N, N+1, \dots, N+n-1$. Hence let $U = [u_0^T, u_1^T, \dots, u_{N-1}^T]^T$ and partition (7) according to the enlarged horizon as

$$\begin{bmatrix} y_1 \\ \vdots \\ \frac{Y_1}{Y_2} \\ \vdots \\ y_{N+n-1} \end{bmatrix}, \quad \begin{bmatrix} P_1 \\ P_2 \end{bmatrix} = \begin{bmatrix} CA \\ \vdots \\ CA^{N-1} \\ CA^N \\ \vdots \\ CA^{N+n-1} \end{bmatrix}, \quad (8)$$

$$\begin{bmatrix} H_1 \\ H_2 \end{bmatrix} = \begin{bmatrix} CB & 0 & \cdots & \cdots & 0 \\ CAB & CB & \cdots & \cdots & 0 \\ \vdots & \vdots & \ddots & \vdots & \vdots \\ \frac{CA^{N-2}B}{CA^{N-1}B} & \frac{CA^{N-3}B}{CA^{N-2}B} & \ddots & \ddots & 0 \\ CA^{N-1}B & CA^{N-2}B & \cdots & \ddots & CB \\ CA^N B & CA^{N-1}B & \cdots & \cdots & CAB \\ \vdots & \vdots & \vdots & \vdots & \vdots \\ CA^{N+n-2}B & CA^{N+n-3}B & \cdots & \cdots & CA^{n-1}B \end{bmatrix} \quad (9)$$

The constraints can be written in the compact form

$$P_2 x_0 + H_2 U = 0 \quad (10)$$

Assuming $\lambda_i = \lambda = \text{const}$ and denoting the Lagrange multiplicator by

$\mu \in R^n$, the Lagrange multiplier rule yields

$$\begin{aligned} L &= \frac{1}{2} \langle P_1 x_0 + H_1 U, P_1 x_0 + H_1 U \rangle + \frac{1}{2} \lambda \langle U, U \rangle + \langle \mu, P_2 x_0 + H_2 U \rangle = \\ &= \frac{1}{2} \langle P_1^T P_1 x_0, x_0 \rangle + \langle H_1^T P_1 x_0, U \rangle + \frac{1}{2} \langle H_1^T H_1 U, U \rangle + \\ &\quad \frac{1}{2} \lambda \langle U, U \rangle + \langle P_2^T \mu, x_0 \rangle + \langle H_2^T \mu, U \rangle \end{aligned} \quad (11a)$$

$$\frac{dL}{dU} = H_1^T P_1 x_0 + \underbrace{(H_1^T H_1 + \lambda I)}_{L_1} U + H_2^T \mu = 0, \quad (11b)$$

$$U = -L_1^{-1}(H_1^T P_1 x_0 + H_2^T \mu), \quad (11c)$$

$$\mu = L_\mu^{-1}(P_2 - H_2 L_1^{-1} H_1^T P_1) x_0. \quad (11d)$$

Hence the optimal control sequence is

$$U = -\underbrace{L_1^{-1}\{H_1^T P_1 + H_2^T L_\mu^{-1}(P_2 - H_2 L_1^{-1} H_1^T P_1)\}}_K x_0 =: -K x_0, \quad (12)$$

where $L_1 = H_1^T H_1 + \lambda I$ and $L_\mu = H_2 L_1^{-1} H_2^T$. The first dim (u) = r row of K will be denoted by \hat{K} , and the optimal predictive control law in closed loop will be the state feedback $u_0 = -\hat{K}x_0$.

2.2. LTV Approximation of Non-linear Mechatronical Systems in the Neighbourhood of Reference Trajectories

We will apply discrete time predictive control based on LTV approximation of the nonlinear system along the reference trajectory hence the first question is the necessary value of the sampling time T for the discrete time LTV system. Denote $x_0(t)$, $u_0(t)$ a feasible reference trajectory for a nonlinear system:

$$\dot{x}_0(t) = f(x_0(t), u_0(t)) \quad (13)$$

Let $\delta x(t)$, $\delta u(t)$ be arbitrary small perturbations of the nonlinear system near the given reference trajectory then

$$\dot{x}(t) = f(x(t), u(t)) \approx f(x_0(t), u_0(t)) + f'_x(x_0(t), u_0(t))\delta x(t) + f'_u(x_0(t), u_0(t))\delta u(t) \quad (14)$$

$$\delta x(t) = x(t) - x_0(t), \quad \frac{d\delta x(t)}{dt} = \dot{x}(t) - \dot{x}_0(t) \quad (15a)$$

$$\frac{d\delta x(t)}{dt} = f'_x(x_0(t), u_0(t))\delta x(t) + f'_u(x_0(t), u_0(t))\delta u(t) \quad (15b)$$

Let us switch from continuous to discrete time using Euler approximation then

$$\delta x_{i+1} = \delta x_i + T f'_x \delta x_i + T f'_u \delta u_i \quad (16)$$

where T is the sampling time for the LTV approximation. In order to find the necessary sampling time T a practical approach may be to connect the reference control $u_0(t)$ through a zero order hold element (ZOH) with tact time T onto the input of the discrete time nonlinear system and check whether the state $x(t)$ of the discrete time nonlinear system remains in the neighbourhood of $x_0(t)$ within the prescribed accuracy.

We restrict us in the sequel for mechatronical systems of the form

$$\tau = H\ddot{q} + h, \dim(q) = n \quad (17)$$

where τ is the torque vector and q is the vector of generalized coordinates, furthermore $u = \tau$ is the input and $x = (q^T, \dot{q}^T)^T$ is the state. For simplicity of the description we assume that the full state is measured: $y = x$ (otherwise deterministic or stochastic observer/estimator is needed). The (dominant part of) state equation has the form

$$\ddot{q}(t) = H^{-1}(q(t))\tau(t) - H^{-1}(q(t))h(x(t)) = f(x, u) \quad (18)$$

For small perturbations at any point of time t :

$$\ddot{q} + \delta\ddot{q} = f(x, u) + \frac{\partial f(x, u)}{\partial q}\delta q + \frac{\partial f(x, u)}{\partial \dot{q}}\delta\dot{q} + \frac{\partial f(x, u)}{\partial u}\delta u \quad (19a)$$

$$\delta\ddot{q} = \left(\frac{\partial H^{-1}}{\partial q}u - \frac{\partial H^{-1}}{\partial q}h - H^{-1}\frac{\partial h}{\partial q} \right)\delta q - H^{-1}\frac{\partial h}{\partial \dot{q}}\delta\dot{q} + H^{-1}\delta u \quad (19b)$$

$$\delta\ddot{q} = \underbrace{\left[\begin{array}{cc} \frac{\partial H^{-1}}{\partial q}(u - h) - H^{-1}\frac{\partial h}{\partial q} & -H^{-1}\frac{\partial h}{\partial \dot{q}} \end{array} \right]}_{A(t)}\delta x + \underbrace{H^{-1}}_{B(t)}\delta u \quad (19c)$$

So $\delta\ddot{q}$ can be written in the following continuous time LTV form:

$$\delta\ddot{q} = A(t)\delta x + B(t)\delta u \quad (20)$$

The horizon length N will be understood in the multiple of sampling time T . Similarly $\delta A_k = A(t_0 + kT)$ and $\delta B_k = B(t_0 + kT)$ where t_0 is the initial time of the moving horizon. The discrete time LTV system for small perturbations can be obtained in the following steps:

$$\delta x_{k+1} = \begin{bmatrix} \delta q_k + T\delta\dot{q}_k \\ \delta\dot{q}_k + T(\underbrace{\delta A_k \delta x_k + \delta B_k \delta u_k}_{\delta\ddot{q}_k}) \end{bmatrix} \quad (21a)$$

$$\delta A_k = [\delta A_{k1}|_{nxn} \quad \delta A_{k2}|_{nxn}] \quad (21b)$$

$$\delta x_{k+1} = \begin{bmatrix} I & TI \\ 0 & I \end{bmatrix} \delta x_k + \begin{bmatrix} 0 \\ T \delta A_k \end{bmatrix} \delta x_k + \begin{bmatrix} 0 \\ T \delta B_k \end{bmatrix} \delta u_k \quad (21c)$$

$$\delta x_{k+1} = \underbrace{\begin{bmatrix} I & TI \\ T \delta A_{k1} & T \delta A_{k2} + I \end{bmatrix}}_{A_k|_{2nx2n}} \delta x_k + \underbrace{\begin{bmatrix} 0 \\ T \delta B_k \end{bmatrix}}_{B_k|_{2nxn}} \delta u_k \quad (21d)$$

This system can be referred in the following compact LTV form:

$$\delta x_{k+1} = A_k \delta x_k + B_k \delta u_k \quad (22)$$

Considering a prediction horizon of size N (in the tact of T) and prescribing the stability condition $\delta x_N = 0$ according to the original suggestion of the Mosca–Zhang method for LTI systems the prediction problem can be formulated as

$$\begin{aligned} \underbrace{\begin{bmatrix} \delta x_1 \\ \delta x_2 \\ \vdots \\ \delta x_N \end{bmatrix}}_{\delta X|_{2Nnx1}} &= \underbrace{\begin{bmatrix} A_0 \\ A_1 A_0 \\ \vdots \\ \prod_{i=N-1}^0 A_i \end{bmatrix}}_P \delta x_0 + \\ &+ \underbrace{\begin{bmatrix} B_0 & 0 & \cdots & 0 \\ A_1 B_0 & B_1 & \cdots & 0 \\ \vdots & \vdots & \ddots & \vdots \\ \left(\prod_{i=N-1}^1 A_i\right) B_0 & \left(\prod_{i=N-1}^2 A_i\right) B_1 & \cdots & B_{k-1} \end{bmatrix}}_Q \delta U_{Nnx1} \quad (23) \end{aligned}$$

$$\delta U = (\delta u_0^T, \delta u_1^T, \dots, \delta u_N^T)^T \quad (24)$$

or in the compact form

$$\delta X = P\delta x_0 + Q\delta U \quad (25)$$

The perturbed trajectory of the system is δX , predicted for an N size horizon, δx_0 is the state perturbation error (with respect to the reference trajectory) in the instantaneous time (at the begin of the actual horizon) and δU is the vector of control signal deviations. The time length of the actual horizon equals $N \cdot T$. The control signal will be determined in every T_c time.

The next question is how to find the horizon length N and sampling time T for prediction purposes. They will be experimentally chosen taking into consideration that the horizon length N limits the accuracy and the stability properties. The reduction of the horizon length (at constant T) causes higher gains (larger control signal), and faster computation time, while the rise causes lower gains and heavier computation time (which limits the choice of T_c). On one hand the sampling time selection has the same effect as the choice of N , but it also defines the accuracy of the prediction.

We have chosen relatively low horizon length N (order 30) for predictive control and relatively moderate sampling time T (order 50ms) for LTV approximation within the horizon in order to assure stability and decrease the computational cost (order $30 \times 50\text{ms} = 1.5\text{s}$ horizon length in time). However the horizon will be moved after every computation by a fine time T_c (order 5ms) so that the new control signal will be computed with high frequency compensating the computational burden and increasing the control bandwidth and accuracy. The reference signal is known at the multiples of T_c .

2.3. Performance Criterions

Different performance criteria can be formulated to be minimized.

Case 1: Minimizing the deviation from the reference trajectory in the prediction horizon without terminal constraint:

$$\begin{aligned} J &= \frac{1}{2} \sum_{i=1}^N \delta x_i^2 \\ J &= \frac{1}{2} \langle \delta X, \delta X \rangle \\ J &= \frac{1}{2} \langle P\delta x_0 + Q\delta U, P\delta x_0 + Q\delta U \rangle \\ \frac{\partial J}{\partial U} &= Q^T P\delta x_0 + Q^T Q\delta U = 0 \end{aligned} \quad (26)$$

The optimal control signal change (the real control signal equals $u_0 + \delta u_0$):

$$\delta U = -\underbrace{(Q^T Q)^{-1} Q^T}_{\text{pseudo inverse}} P \delta x_0$$

Case 2: Minimizing the deviation from the reference trajectory in the prediction horizon with terminal constraint ($\delta x_N := 0$)

$$J = \frac{1}{2} \langle \delta X, \delta X \rangle + \underbrace{\mu}_{\substack{\text{Lagrange} \\ \text{multipliator}}} \langle \delta x_N \rangle \quad (27)$$

$$J = \frac{1}{2} \langle P \delta x_0 + Q \delta U, P \delta x_0 + Q \delta U \rangle + \langle \mu, P_N \delta x_0 + Q_N \delta U \rangle$$

$$P_N = \left[\prod_{i=N-1}^0 A_i \right]_{2nx2n}, \quad Q_N = \left[\begin{array}{cccc} \left(\prod_{i=N-1}^1 A_i \right) B_0 & \left(\prod_{i=N-1}^2 A_i \right) B_1 & \cdots & B_{N-1} \end{array} \right]_{2nxNn}$$

$$\frac{\partial J}{\partial U} = Q^T P \delta x_0 + Q^T Q \delta U + Q_N^T \mu = 0$$

The optimal control signal change:

$$\delta U = -(Q^T Q)^{-1} (Q^T P \delta x_0 + Q_N^T \mu)$$

After substitution in the constraint:

$$\mu = (Q_N (Q^T Q)^{-1} Q_N^T)^{-1} (P_N \delta x_0 - Q_N (Q^T Q)^{-1} Q^T P \delta x_0)$$

Case 3: Minimizing deviation from the reference trajectory and the control signal change in the prediction horizon with terminal constraint ($\delta x_N := 0$)

$$J = \frac{1}{2} \langle \delta X, \delta X \rangle + \langle \mu, \delta x_k \rangle + \frac{1}{2} \lambda \langle \delta U, \delta U \rangle \quad (28)$$

$$\frac{\partial J}{\partial u} = Q^T P \delta x_0 + Q^T Q \delta U + Q_N^T \mu + \lambda I \delta U = 0$$

The optimal control signal change:

$$\delta U = -(Q^T Q + \lambda I)^{-1} (Q^T P \delta x_0 + Q_N^T \mu)$$

After substitution in the constraint:

Table 1. Denavit-Hartenberg parameters of the inverted pendulum PS600

i	q_i	ϑ_i	d_i	a_i	α_i
1	d_1	0	d_1	0	$-\pi/2$
2	ϑ_2	ϑ_2	0	a_2	0

$$\mu = (Q_N(Q^T Q + \lambda I)^{-1} Q_N^T)^{-1} (P_N \delta x_0 - Q_N(Q^T Q + \lambda I)^{-1} Q^T P \delta x_0)$$

Case 4: Integrator state expansion:

$$A_i = \begin{pmatrix} A_{i,1} \\ A_{i,2} \\ \vdots \\ A_{i,2n} \end{pmatrix}, \quad B_i = \begin{pmatrix} B_{i,1} \\ B_{i,2} \\ \vdots \\ B_{i,2n} \end{pmatrix}$$

The equation of the state of the augmented integrator (integral of the j-th state):

$$x_{I_j,i+1} = \begin{pmatrix} T A_{i,j} & I \end{pmatrix} \begin{pmatrix} x_i \\ x_{I_j,i} \end{pmatrix} + (T B_{i,j}) \delta u_i$$

State equation with the new state(s):

$$\begin{pmatrix} x_{i+1} \\ x_{I_j,i+1} \end{pmatrix} = \underbrace{\begin{pmatrix} A_i & 0 \\ T A_{i,j} & I \end{pmatrix}}_{\text{new } A_i \text{ matrix}} \begin{pmatrix} x_i \\ x_{I_j,i} \end{pmatrix} + \underbrace{\begin{pmatrix} B_i \\ T B_{i,j} \end{pmatrix}}_{\text{new } B_i \text{ matrix}} \delta u_i \quad (29)$$

3. Dynamic Model and Energy Based Control Concept for the Inverted Pendulum

As stated earlier the elaborated method for predictive control of nonlinear systems in the neighbourhood of given reference trajectories can be applied both for fully actuated and underactuated systems. In the paper we consider the more challenging problem of predictive control of an underactuated system, the inverted pendulum, which is not flat from differential geometrical point of view.

The inverted pendulum can be divided into cart and rod (pendulum). The Denavit–Hartenberg form of the assumed PS600 inverted pendulum is given in Table 1.

Let us denote $L_s = a_2$ the center of gravity (COG) of the rod, M_l the mass of the rod, Θ the inertia of the rod belonging to COG, M_0 the mass of the chart, F_v the

Table 2. Physical parameters of the inverted pendulum PS600

M0	4	kg
M1	0.36	kg
M=M0+M1	4.36	kg
Ls	0.451	m
θ (respect to cog)	0.0111	kgm^2
θ (respect to pivot point)	0.08433	
Fr	10	kg/s
C	0.00145	kgm^2/s

viscous friction coefficient and F_c the Coulomb friction coefficient, respectively. The physical parameters (all in SI units) of the system are summarized in *Table 2*.

If the positive direction of $q_1 = d_1$ is pointed to the right and the positive direction of the rotation axis of the rod is pointed ‘before the paper’ then the down-right stable equilibrium belongs to $q_2 = \pi$ (or $q_2 = -\pi$) while the upright unstable equilibrium belongs to $q_2 = 0$. The cart is actuated by the force F . Using these directions of the joint variables the motion equations have the form

$$\begin{aligned} (M_0 + M_1)\ddot{q}_1 + M_1L_s \cos(q_2)\ddot{q}_2 - M_1L_s \sin(q_2)\dot{q}_2^2 + f_{1\text{friction}} &= F \\ M_1L_s \cos(q_2)\ddot{q}_1 + (\Theta + M_1L_s^2)\ddot{q}_2 - M_1L_s g \sin(q_2) + f_{2\text{friction}} &= 0 \end{aligned} \quad (30)$$

and therefore

$$\begin{aligned} H &= \begin{bmatrix} M_0 + M_1 & M_1L_s \cos(q_2) \\ M_1L_s \cos(q_2) & \Theta + M_1L_s^2 \end{bmatrix} = \begin{bmatrix} 4.36 & 0.1624 \cos(q_2) \\ 0.1624 \cos(q_2) & 0.08432 \end{bmatrix} \\ h &= \begin{pmatrix} -M_1L_s \sin(q_2)\dot{q}_2^2 \\ -M_1L_s g \sin(q_2) \end{pmatrix} + f_{\text{friction}} = \begin{pmatrix} -0.1624 \sin(q_2)\dot{q}_2^2 \\ -1.593 \sin(q_2) \end{pmatrix} + f_{\text{friction}} \end{aligned} \quad (31)$$

Since the system is underactuated the reference path is constrained by the second equation of (30) which can not be integrated in closed form. Hence reference path design is a nontrivial problem.

For swinging up the pendulum Åström and Furuta [9] have elaborated an energy based approach. Denoting by $J := \Theta + M_1L_s^2$ the inertia of the pivot and introducing normalized variables $\omega_0 := \sqrt{M_1gL_s/J}$, $\tau := \sqrt{M_1gL_s/J}t$, $v := u/g$ and $u_{\max} := \max|u| = ng$ where u is the acceleration of the pivot of the pendulum, the constraint part of the motion equation and the normalized total energy $E_n := E/(mgl)$ of the uncontrolled subsystem can be written in the following form (for simplicity in the sequel we introduce $\vartheta := q_2$, $m := M_1$ and

$l := L_s$, moreover the friction is neglected):

$$\begin{aligned} \frac{d^2\vartheta}{d\tau^2} - \sin\vartheta + v \cos\vartheta &= 0 \\ E_n = \frac{1}{2} \left(\frac{d\vartheta}{d\tau} \right)^2 + \cos\vartheta - 1. \end{aligned} \quad (32)$$

The system is thus characterized by two parameters only, the natural frequency for small oscillations ω_0 and the normalized maximum acceleration of the pendulum $n = u_{\max}/g$ where the latter is limited by the drive system and power electronics of the inverted pendulum. The swinging up problem can be solved by controlling the energy. The basic idea is that in order to swing up the pendulum to the upright position an energy is to be given to the system which corresponds to the upright position. This corresponds to the trajectory

$$E = \frac{1}{2} J \dot{\vartheta}^2 + mgl(\cos\vartheta - 1) = 0 \quad (33)$$

hence performing energy control

$$\frac{dE}{dt} = J \dot{\vartheta} \ddot{\vartheta} - mgl \dot{\vartheta} \sin\vartheta = -mnl \dot{\vartheta} \cos\vartheta \quad (34)$$

should be satisfied. A control strategy can be obtained based on the Lyapunov function $V = (E - E_0)^2/2$ and the control law

$$u = k(E - E_0)\dot{\vartheta} \cos\vartheta \quad (35)$$

resulting in

$$\frac{dV}{dt} = -mlk((E - E_0)\dot{\vartheta} \cos\vartheta)^2. \quad (36)$$

The Lyapunov function decreases as long $\dot{\vartheta} \neq 0$ and $\cos\vartheta \neq 0$. To change the energy as fast as possible the control signal should be as large as possible which is achieved by the control law

$$u = ng \cdot \text{sign}((E - E_0)\dot{\vartheta} \cos\vartheta) \quad (37)$$

driving V to zero and E toward E_0 . Control chattering may arise which can be avoided if

$$u = \text{sat}_{ng}((k(E - E_0) \text{sign}(\dot{\vartheta} \cos\vartheta)). \quad (38)$$

The swinging up behaviour can be characterized by the following equation describing the number of swings k :

$$2 \sin\vartheta_0 \geq 1 = \cos((2k - 1)\vartheta_0) \quad (39)$$

where $n = \tan \vartheta_0$. The solution of the inequality defines the relation between the acceleration of the pivot n and the number of swings k . For small values of n the relation is approximately given by $n \approx \pi/(2k - 1)$. Single swing behaviour requires that $n > 4/3$, double swing behaviour that $n > 0.577$. [9]

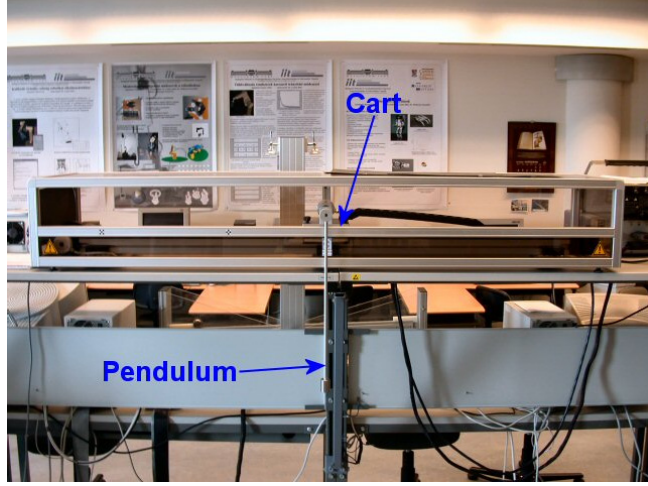


Fig. 1.

The reference path design for the swinging up period has been performed in the paper by using the above energy based method.

4. Predictive Control of the Inverted Pendulum

The energy based algorithm for reference path design in the swing up period and the predictive control algorithm based on the LTV model for perturbations around the reference path were programmed in MATLAB and C, furthermore a simulation framework was developed in MATLAB/Simulink for the testing of the control method. The reference path was taken into consideration as feedforward compensation to which the predictive control component was added in closed loop. After exhaustive examination of the control behavior, the algorithm was applied to a real system, the inverted pendulum PS600 [10], see *Fig. 1*.

The system is controlled by a Quanser Q8 card, with WinCon software under Windows [11]. The WinCon uses Venturcom RTX real-time kernel for Windows, so the timing specifications can be met. The computer used for the control was equipped with Intel Pentium 4 2.8GHz CPU.

The system is started in the downright stable position, reference path for the swing up was designed based on the nonlinear model of the pendulum and the energy approach. The states and the control signals were recorded during

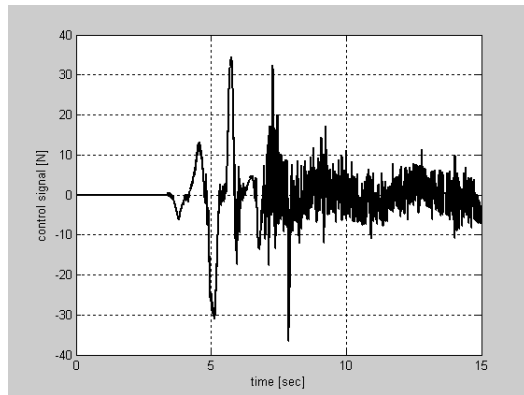


Fig. 2. Control signal, $T=0.04$ s continuous: realized, dashed: reference

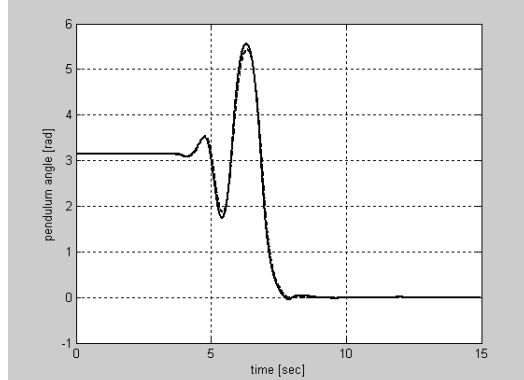


Fig. 3. Angle of the pendulum, $T=0.04$ s

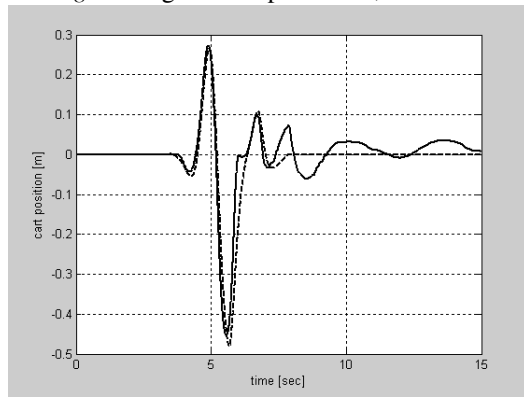


Fig. 4. Cart position without integrator $T=0.04$ s continuous: realized, dashed: reference

the simulation and were used as reference during the swing up phase of the real system. The stabilization of the pendulum around the upright (or downright) equilibrium does not require a complex reference trajectory, since the working point $x_0 = (0 \ 0 \ 0 \ 0)^T$, $u_0 = 0$ is feasible. So the reference trajectory contains only one state. This means that during the stabilization of the pendulum the controller behaves as a linear predictive control, since the reference is x_0, u_0 along the prediction horizon, so the A and B matrices are constant.

For the control of the real system $T_c = 0.005$ s sampling time, for the prediction process and LTV linearization $T = 0.04$ s and $T = 0.05$ s prediction step sizes and $N = 30$ horizon length were chosen (the hardware setup can calculate the algorithm with the above described parameters in the order of 3ms). Experimental results based on the predictive control of the nonlinear underactuated system are summarized in *Figs. 2-7*.

A video can be downloaded from web.axelero.hu/thesis/DSCN0538.MOV. The video needs QuickTime Player to be installed in order to play correctly.

During the experiment switching between controllers for swinging up and stabilization is not needed. The swinging up phase is realized by using energy control and as a consequence of the theory and the physical properties of the system it necessarily contains multiple left and right movements which are not oscillations from theoretical point of view. The end of the swinging up phase is approximately at $t = 8$ s. The significant oscillation at the beginning of the stabilization is caused by the small step in the reference signal. The trajectory generated by the simulation based on energy concept was truncated at this time point, where the state was close to x_0 (the upright unstable equilibrium). After that the reference signal consists of the vector x_0 hence there is a small jump also in the trajectory of the state.

Fig. 2 shows the control signal for $T = 0.04$ s (without integrator states). The high amplitude chattering in the stabilization phase is caused by the high gain as a consequence of the relatively small horizon length (1.2s) and the unmodelled static friction which is large for the cart and small for the pendulum. This can be seen in Figure 3, where the angle of the pendulum is shown. Notice that the reference and the realized trajectories are almost identical, what is due to the fact that the model of the pendulum is very close to the physical reality because of small friction.

The rest of the figures show only the cart position. In *Figs. 4-5* one can see the position of the cart for $T=0.04$ s and $T=0.05$ s. The two cases do not differ much, but the overall error is smaller in the case of higher gain (smaller horizon length). *Figs. 6-7* show the cart position similar to *Figs. 4-5*, but with integrator states. The error between the reference and the realized trajectory is smaller except at the beginning of the stabilization phase. In the neighbourhood of the small jump in the reference signal the (positive or negative) error in the horizon will be integrated and it can only be compensated by transients with opposite error sign which causes oscillation while the horizon surrounds the jump. Because of the same reason the perturbation is almost symmetrical to the reference signal (what is not the case in *Figs. 4-5*). After this the error vanishes quickly, of course depending on the value of T .

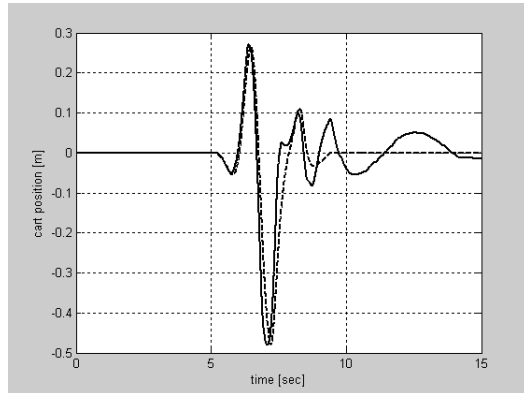


Fig. 5. Cart position without integrator $T=0.05\text{s}$ continuous: realized, dashed: reference

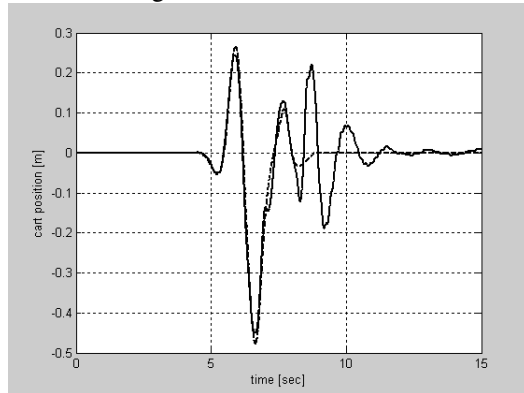


Fig. 6. Cart position with integrator $T=0.04\text{s}$ continuous: realized, dashed: reference

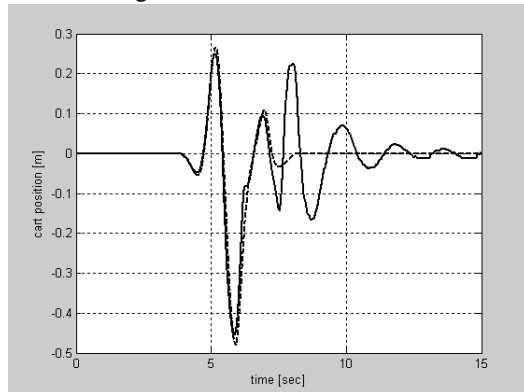


Fig. 7. Cart position with integrator $T=0.05\text{s}$ continuous: realized, dashed: reference

5. Conclusion

The state space predictive control algorithm of Mosca–Zhang has been generalized for underactuated perturbed nonlinear systems along known reference trajectories. The developed method was applied for the control of the inverted pendulum by using quick prototyping software design tools and embedded control architecture. Additional integrators were used to damp the oscillation of the car near the unstable equilibrium.

Acknowledgement

Support for the research of predictive control of underactuated systems was provided by the Hungarian National Research Program under grant No. T 042634 and by the Control System Research Group of the Hungarian Academy of Sciences.

References

- [1] CAMACHO, E. F. – BORDONS, C., *Model predictive control*. Springer, London, (2000).
- [2] ROSSITER, J. A. – KOUVARATAKIS, B. – RICE, M. J., (1998). A Numerically Robust State-space Approach to Stable-predictive Control Strategies . *Automatica*, **34**, pp. 65–73.
- [3] LANTOS, B. (2003). *Control systems theory and design. Vol. II. Advanced control systems* (in Hungarian). Hungarian Academic Press, Budapest.
- [4] ALLGÖWER, F. – ZHENG, A. ed. *Nonlinear Predictive Control*. Birkhäuser, Basel, 2000.
- [5] KIM, H.J. – D. H. SHIM, A Flight Control System for Aerial Robots. *Control Engineering Practice*, **11**, (2003), pp. 1389–1400.
- [6] YU, J. – JADBABQIE, A. – JIMBS, J. – HUANG, Y. Comparison of Nonlinear Control Design Techniques on a Model of the Caltech Ducted Fan. *Automatica*, **37**, (2001), pp. 1971–1978.
- [7] MOSCA , E. – ZHANG, J. Stable Design of Predictive Control. *Automatica*, **28**, (1992), pp. 1229–1233.
- [8] RAWLINGS, J.B. – MUSKE, K.R., The Stability of Constrained Receding Horizon Control. *IEEE Trans. Automatic Control*, **38**, (1993), pp. 1512–1516.
- [9] ÅSTRÖM, K. J. – FURUTA, K., Swinging up a Pendulum by Energy Control, *Automatica*, **36**, (2000), pp. 287–295.
- [10] PS600 Laboratory Experiment Inverted Pendulum, Amira GmbH, 2000.
- [11] Quanser Q8 Data Acquisition System, Quanser, 2003.